ChemComm

RSC Publishing

COMMUNICATION

View Article Online
View Journal | View Issue

TiO_2 nanotube arrays: intrinsic peroxidase mimetics†

Lingling Zhang,‡ Lei Han,‡ Peng Hu, Li Wang and Shaojun Dong*

Cite this: *Chem. Commun.*, 2013, **49**, 10480

Received 12th August 2013,
Accepted 9th September 2013

DOI: 10.1039/c3cc46163g

www.rsc.org/chemcomm

TiO_2 nanotube arrays (NTA), prepared by potentiostatic anodization, were discovered to possess an intrinsic peroxidase-like activity. The colorimetric and electrochemical assays both demonstrated their excellent catalytic activity towards H_2O_2 reduction. On this basis, a simple and inexpensive electrochemical biosensor for glucose detection was developed.

In the past few decades, TiO_2 has been extensively studied as an advanced material in various fields such as photocatalysis, dye-sensitized solar cells, electrochemistry and biomedical devices.[1] Among its various geometries, TiO_2 nanotube arrays (NTA) have gained increasing interest because of the unique combination of the highly functional features of TiO_2 with a regular and controllable nanoscale geometry (length, tube diameter, and self-ordering can be adjusted over large length scales).[1b,2] For instance, P. Schmuki's group reported a series of applications of TiO_2 NTA such as photocatalysis, dye-sensitized solar cells, cancer cell killing and controllable drug delivery.[2d–f,i] Also, TiO_2 NTA is widely used as an efficient carrier due to its considerable support effects to some electrocatalysts, such as horseradish peroxidase,[3] metal Ni[4] and platinum nanoparticles.[5] Nevertheless, in terms of the intrinsic peroxidase mimetics of TiO_2 NTA itself, it has not been explored to the best of our knowledge. As we know, great attention has been paid to the construction and discovery of novel enzyme mimetics since the use of natural enzymes brings up issues regarding the cost of production and reaction conditions.[6] Most of the research studies have focused on peroxidase mimetics such as hemin and DNAzymes.[6] Until recently, some metal oxide nanomaterials have also been found to exhibit peroxidases-like activity similar to that found in natural peroxidases, *i.e.* Fe_3O_4 magnetic nanoparticles (NPs) and their surrounding derivatives,[7,8] Co_3O_4 nanoparticles (NPs)[9] and V_2O_5 nanowires.[10] However, their preparation and protocols reported so far are complex, and/or the reaction temperature is high, moreover, it is generally very hard to recycle such catalysts by centrifugation, which significantly limits their practical applications.

Herein we discovered for the first time that TiO_2 NTA prepared by the anodization of titanium possessed intrinsic peroxidase-like activity, which could catalyze the oxidation of different peroxidase substrates, such as TMB, OPDA, and ABTS, in the presence of H_2O_2. TiO_2 NTA has the advantages of high stability, efficiency, controlled preparation at low cost, easy separation and re-utilization in comparison to natural HRP. Moreover, TiO_2 NTA could be simply used as a working electrode owing to the nanotube directly grown on the metal substrate, and was found to exhibit excellent electrocatalytic activity towards H_2O_2 reduction. Combining with glucose oxidase (GOD) an electrochemical glucose biosensor was successfully developed, which exhibited excellent selectivity, stability and reusability.

TiO_2 NTA synthesis and characterization are shown in the Fig. S1 (ESI†). Under experimental conditions, TiO_2 NTA can catalyze the oxidation of TMB by H_2O_2 to produce the typical blue color reaction with maximum absorbance at 652 nm (shown in Fig. 1A), which originates from the oxidation of TMB.[9] Nevertheless, the TMB + H_2O_2 system without TiO_2 NTA was colorless and the one with the Ti foil system showed slight color variation. We also repeated the experiments using ABTS and OPDA. Fig. 2 shows that TiO_2 NTA not only catalyzed oxidation of TMB producing a blue color, but also catalyzed ABTS to give a green color and OPDA to give an orange color. At the same time, the electrocatalytic activity of TiO_2 NTA and

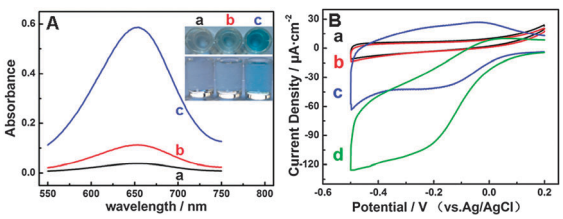

Fig. 1 (A) The absorption spectra and digital photos of colorimetric reaction of TMB and H_2O_2 in 0.1 M pH 3.5 NaAc buffer solutions without catalyst (a), with Ti foil (b) and TiO_2 NTA (c) as the catalysts; (B) cyclic voltammograms (CVs) obtained at Ti foil (a, b) and the TiO_2 NTA (c, d) electrode in 0.1 M pH 5.5 PBS without (a, c) and with (b, d) 0.3 mM H_2O_2. Scan rate is 50 mV s^{-1}.

State Key Laboratory of Electroanalytical Chemistry, Changchun Institute of Applied Chemistry, Chinese Academy of Sciences, Changchun 130022, P.R. China. E-mail: dongsj@ciac.jl.cn; Fax: +86 431-85689711; Tel: +86 431-85262101

† Electronic supplementary information (ESI) available. See DOI: 10.1039/c3cc46163g

‡ These authors contributed equally to this work.

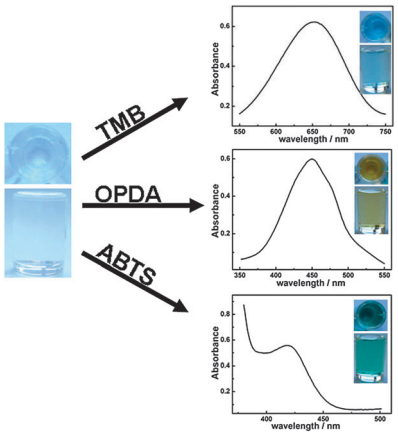

Fig. 2 The absorption spectra and digital photos of colorimetric reaction of TMB, OPDA and ABTS oxidation by H_2O_2 in 0.1 M pH 3.5 NaAc buffer solutions with TiO_2 NTA as the catalyst.

Ti foil towards H_2O_2 reduction was compared (Fig. 1B). Obviously, the TiO_2 NTA electrode exhibits high electrocatalytic activity towards H_2O_2 reduction with an onset potential of 0.15 V and a maximum reduction current of 60 μA cm^{-2} at −0.25 V (curve d), while the reduction current could hardly be observed in Ti foil. This indicates that TiO_2 NTA could facilitate the electron transfer between the electrode and H_2O_2. It is thought that the TiO_2 NTA could also have the ability to transfer electrons between TMB and H_2O_2, increasing the reaction rate of TMB oxidation catalyzed by TiO_2 NTA.[9] Such excellent performance of TiO_2 NTA may be attributed to the following reasons: the highly ordered nanotubular architecture of TiO_2 NTA not only presents a large specific surface area but also provides a one-dimensional electronic channel and reduces the grain boundaries.[11] Both the colorimetric and electrochemical methods indicated that the peroxidase-like activity towards H_2O_2 is contributed from TiO_2 NTA rather than the Ti metal.

In addition, considering that TiO_2 NTA is widely used in the field of photoelectrochemistry, the influence of light illumination on the electrocatalytic activity of the TiO_2 NTA electrode was also examined. The results displayed in Fig. S2 (ESI†) suggest that the electron–hole separation caused by UV light illumination favors water oxidation instead of H_2O_2 reduction.

As expected, like HRP, the catalytic activity of TiO_2 NTA is also dependent on temperature, pH, and H_2O_2 concentration. The peroxidase-like activity of TiO_2 NTA was measured by varying the pH from 2 to 12, the temperature from 15 °C to 65 °C, and the H_2O_2 concentration from 0.001 to 20 mM. It can be found that TiO_2 NTA exhibits the maximum catalytic activity under the following optimal conditions: pH 3.5, 40 °C, and 3 mM H_2O_2, which are close to the values for other NP-based peroxidase mimetics and HRP (Fig. S5, ESI†).[7,9,12] Therefore, we adopted these optimal conditions for subsequent analysis of TiO_2 NTA activity.

The peroxidase-like catalytic property of TiO_2 NTA was further investigated using steady-state kinetics under standard conditions. Within a suitable range of substrate concentration the reaction was consistent with typical Michaelis–Menten kinetics for both TiO_2 NTA (Fig. S6A and B, ESI†) and HRP (Fig. S6C and D, ESI†). V_{max} and K_m were calculated from Lineweaver–Burk plots and are listed in Table 1. The K_m value of TiO_2 NTA with H_2O_2 as the substrate is

Table 1 Comparison of the Michaelis–Menten constant (K_m) and maximum reaction rate (V_{max}) between TiO_2 NTA and HRP

Catalysts	Substrate	K_m/mM	$V_{max}/10^{-8}$ M s^{-1}
TiO_2 NTA	TMB	0.127	7.02
TiO_2 NTA	H_2O_2	5.26	760
HRP	TMB	0.123	14.5
HRP	H_2O_2	7.08	491

close to that of HRP. Generally, K_m is identified as an indicator of enzyme affinity to substrates. So the similar K_m values of TiO_2 NTA and HRP proved that the affinity of TiO_2 NTA to its substrate is close to that of HRP and would result in high activities and wide-range applications. Moreover, we compared the K_m value of TiO_2 NTA towards H_2O_2 in the present work with that of other traditional mimic enzymes, such as Fe_3O_4 MNPs, graphene oxide, carbon nanodots and CO_3O_4 NPs, which are listed in Table S1 in the ESI.† The table shows the higher affinity of TiO_2 NTA to the substrate, H_2O_2, than most of the other peroxidase-like nanomaterials. In addition, the similar K_m values for TMB indicate the same affinity of TiO_2 NTA and HRP for TMB. The double-reciprocal plots (Fig. S6E and F, ESI†) revealed the characteristic parallel lines of a ping-pong mechanism and implied that, like HRP, TiO_2 NTA binds and reacts with the first substrate, and then releases the first product before reacting with the second substrate.

The stability of TiO_2 NTA in wide pH and temperature ranges is crucial to extend their applications, thus we expect it to be more stable than the natural enzyme HRP. To certify this, we first incubated both HRP and TiO_2 NTA at a wide range of pH values and temperatures for 2 h, and then measured their activities under standard conditions. The catalytic activity of HRP was largely inhibited after incubation at pH lower than 5 or temperature higher than 40 °C. In contrast, the catalytic activity of TiO_2 NTA remained stable after treatment under the same conditions (Fig. S7, ESI†). The robustness of TiO_2 NTA makes them suitable for a broad range of applications in the biomedicine and environmental chemistry fields.

On the basis of the intrinsic peroxidase-like property of TiO_2 NTA, we developed a simple electrochemical method to detect H_2O_2 and glucose. Fig. 3A shows the amperometric response at the TiO_2 NTA electrode to an aliquot of 10 μM H_2O_2 for each step in 0.1 M pH 5.5 PBS under a constant potential of −0.25 V and the fitted relationship between the current and H_2O_2 concentration in the inset. A wide linear response range from 200 nM to 100 μM (R = 0.999) was obtained with the sensitivity of 240 μA cm^{-2} mM^{-1} and a fast response time of 5 s. The detection limit is calculated to be 50 nM corresponding to 3 times the noise. The relative standard deviation (RSD) for 5 successive determinations was 1.3%, suggesting good stability and reproducibility. Also, specificity is an essential factor for the artificial enzymes. Some electroactive species are widely known as the interferents in H_2O_2 detection, especially AA, DA, and UA. In Fig. 3B, 2 mM DA and 2 mM UA show no obvious influence on the reduction current of H_2O_2, while the reduction current decreases slightly with the addition of 2 mM AA. The possible reason is that AA is a strong reductant and its reaction at −0.25 V disturbs H_2O_2 reduction. Since the response to 2 mM AA is far less than the one to equal concentration of H_2O_2, the specificity of the TiO_2 NTA electrode was regarded as acceptable and reasonable.

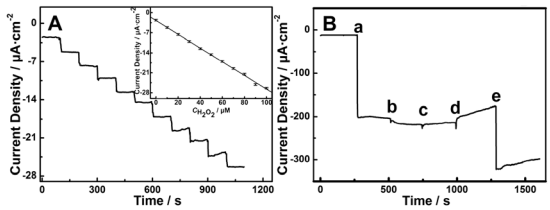

Fig. 3 (A) Amperometric response obtained at the TiO_2 NTA electrode in 0.1 M pH 5.5 PBS upon successive injection of 10 μM H_2O_2 for each step at −0.25 V, the inset is the fitted current plot *versus* H_2O_2 concentration; (B) amperometric response at the TiO_2 NTA electrode in 0.1 M pH 5.5 PBS at −0.25 V with sequential injection of 2 mM H_2O_2 (a), 2 mM UA (b), 2 mM DA (c), 2 mM AA (d) and 2 mM H_2O_2 (e).

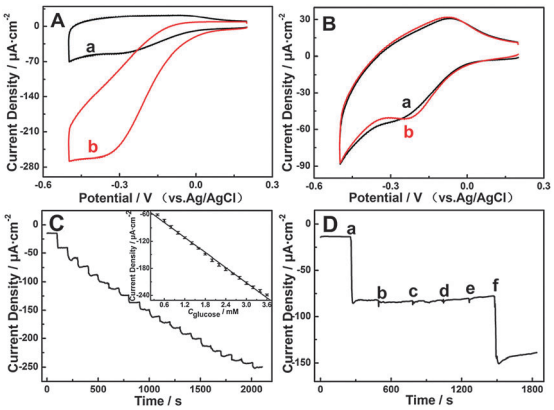

Fig. 4 (A) CVs obtained at the GOD/TiO_2 NTA electrode in 0.1 M pH 5.5 PBS without (a) and with (b) 4 mM glucose; (B) CVs obtained at the TiO_2 NTA electrode in 0.1 M pH 5.5 PBS without (a) and with (b) 4 mM glucose; (C) amperometric response obtained at the GOD/TiO_2 NTA electrode in 0.1 M pH 5.5 PBS upon successive injection of 0.2 mM glucose for each step at −0.35 V, the inset is the linear fitted current plot to glucose concentration; (D) amperometric response at the GOD/TiO_2 NTA electrode in 0.1 M pH 5.5 PBS at −0.35 V with sequential injection of 1 mM glucose (a), 2 mM fructose (b), 2 mM lactose (c), 2 mM sucrose (d), 2 mM maltose (e), and 1 mM glucose (f).

Glucose detection is a common analysis in the clinic and the laboratory. Generally, glucose oxidase catalyzes the oxidation of glucose to produce gluconic acid and hydrogen peroxide in the presence of oxygen. Therefore, a glucose biosensor was successfully constructed through coupling TiO_2 NTA with GOD. Here, GOD was immobilized into the TiO_2 NTA electrode by simple physical adsorption. The current responding to 5 mM glucose at the as-prepared GOD/TiO_2 NTA electrode reaches 216 μA cm^{-2} at −0.35 V (Fig. 4A). As a control, a TiO_2 NTA electrode without GOD modification was employed to catalyze glucose oxidation. No catalytic current can be observed upon glucose addition (Fig. 4B). Amperometric responses at the GOD/TiO_2 NTA electrode to successive addition of aliquots of 0.2 mM glucose at a constant potential of −0.35 V are shown in Fig. 4C. The average response time is 8 s and the LOD is 5 μM. From the inset of Fig. 4C, it can be seen that the sensitivity for glucose detection is 56.7 μA cm^{-2} mM^{-1} and the linear detection range is from 0.4 mM to 3.6 mM (R = 0.998). The RSD for 5 successive determinations is 3.7%. For testing the anti-interference ability of the glucose biosensor, fructose, lactose, sucrose, and maltose of 2 mM, respectively, were selected as the possible interferents. All these species have no influence on the catalytic current (Fig. 4D), which suggests an excellent selectivity of the developed glucose biosensor. In real sample assays, the blood glucose concentration of diabetes patients was measured as 8.23 ± 0.05 mM (n = 3) according to the amperometric response to the diluted serum, which coincides with the results (8.0 mM) given by the hospital. Moreover, the GOD/TiO_2 NTA electrode could be easily refreshed by rinsing with water and then immersing in a GOD solution.

In summary, we first discovered that TiO_2 NTA possessed intrinsic peroxidase-like activity. Kinetic analyses confirmed that the catalysis was in accordance with typical Michaelis–Menten kinetics and followed a ping-pong mechanism. In addition, the TiO_2 NTA electrode showed excellent electrocatalytic activity towards H_2O_2 reduction with a LOD of 50 nM. On this basis, a simple and inexpensive electrochemical glucose biosensor was developed. Nonetheless, there are some challenges to be addressed, such as low efficiency and poor selectivity. Thus many efforts need to be made in the future and the breakthrough in this field will lead to a new wave of novel biocatalysts which could find wide applications in biotechnology and clinical diagnosis as enzymatic mimetics.

This work is supported by the National Natural Science Foundation of China (Nos. 20935003 and 21075116) and the 973 Projects (2010CB933603 and 2011CB911002).

Notes and references

1 (*a*) X. Chen, L. Liu, P. Y. Yu and S. S. Mao, *Science*, 2011, **331**, 746–750; (*b*) P. Roy, S. Berger and P. Schmuki, *Angew. Chem., Int. Ed.*, 2011, **50**, 2904–2939; (*c*) G. Wang, H. Wang, Y. Ling, Y. Tang, X. Yang, R. C. Fitzmorris, C. Wang, J. Z. Zhang and Y. Li, *Nano Lett.*, 2011, **11**, 3026–3033; (*d*) Y. B. Tang, C. S. Lee, J. Xu, Z. T. Liu, Z. H. Chen, Z. He, Y. L. Cao, G. Yuan, H. Song, L. Chen, L. Luo, H. M. Cheng, W. J. Zhang, I. Bello and S. T. Lee, *ACS Nano*, 2010, **4**, 3482–3488.

2 (*a*) L. Han, L. Bai, C. Zhu, Y. Wang and S. Dong, *Chem. Commun.*, 2012, **48**, 6103–6105; (*b*) G. K. Mor, K. Shankar, M. Paulose, O. K. Varghese and C. A. Grimes, *Nano Lett.*, 2005, **6**, 215–218; (*c*) X. Quan, S. Yang, X. Ruan and H. Zhao, *Environ. Sci. Technol.*, 2005, **39**, 3770–3775; (*d*) J. R. Jennings, A. Ghicov, L. M. Peter, P. Schmuki and A. B. Walker, *J. Am. Chem. Soc.*, 2008, **130**, 13364–13372; (*e*) M. Kalbacova, J. M. Macak, F. Schmidt-Stein, C. T. Mierke and P. Schmuki, *Phys. Status Solid RRL*, 2008, **2**, 194–196; (*f*) Y. Y. Song, F. Schmidt-Stein, S. Bauer and P. Schmuki, *J. Am. Chem. Soc.*, 2009, **131**, 4230–4232; (*g*) Y. C. Nah, I. Paramasivam and P. Schmuki, *ChemPhysChem*, 2010, **11**, 2698–2713; (*h*) N. K. Shrestha, J. M. Macak, F. Schmidt-Stein, R. Hahn, C. T. Mierke, B. Fabry and P. Schmuki, *Angew. Chem., Int. Ed.*, 2009, **48**, 969–972; (*i*) J. M. Macak, M. Zlamal, J. Krysa and P. Schmuki, *Small*, 2007, **3**, 300–304.

3 S. Liu and A. Chen, *Langmuir*, 2005, **21**, 8409–8413.

4 C. Wang, L. Yin, L. Zhang and R. Gao, *J. Phys. Chem. C*, 2010, **114**, 4408–4413.

5 Y. Song, Z. Gao, K. Lee and P. Schmuki, *Electrochem. Commun.*, 2011, **13**, 1217–1220.

6 (*a*) Q. Wang, Z. Yang, X. Zhang, X. Xiao, C. K. Chang and B. Xu, *Angew. Chem., Int. Ed.*, 2007, **46**, 4285–4289; (*b*) S. Tang, P. Tong, H. Li, F. Gu and L. Zhang, *Biosens. Bioelectron.*, 2013, **41**, 397–402; (*c*) H. Sun, X. Li, Y. Li, L. Fan and H.-B. Kraatz, *Analyst*, 2013, **138**, 856–862; (*d*) F. Li, L. Yang, M. Chen, Y. Qian and B. Tang, *Biosens. Bioelectron.*, 2013, **41**, 903–906; (*e*) M. Sono, M. P. Roach, E. D. Coulter and J. H. Dawson, *Chem. Rev.*, 1996, **96**, 2841–2888.

7 L. Gao, J. Zhuang, L. Nie, J. Zhang, Y. Zhang, N. Gu, T. Wang, J. Feng, D. Yang, S. Perrett and X. Yan, *Nat. Nanotechnol.*, 2007, **2**, 577–583.

8 Y. Dong, H. Zhang, Z. Rahman, L. Su, X. Chen, J. Hu and X. Chen, *Nanoscale*, 2012, **4**, 3969–3976.

9 J. Mu, Y. Wang, M. Zhao and L. Zhang, *Chem. Commun.*, 2012, **48**, 2540–2542.

10 R. André, F. Natálio, M. Humanes, J. Leppin, K. Heinze, R. Wever, H. C. Schröder, W. E. G. Müller and W. Tremel, *Adv. Funct. Mater.*, 2011, **21**, 501–509.

11 L. Xing, J. Jia, Y. Wang, B. Zhang and S. Dong, *Int. J. Hydrogen Energy*, 2010, **35**, 12169–12173.

12 W. Shi, Q. Wang, Y. Long, Z. Cheng, S. Chen, H. Zheng and Y. Huang, *Chem. Commun.*, 2011, **47**, 6695–6697.

